

# Supporting Information

## Flexible and Precise Droplet Manipulation by a Laser-Induced Shape Temperature Field on a Lubricant-Infused Surface

*Xiaoyan Sun<sup>1</sup>, Dejian Kong<sup>1</sup>, Chang Liang<sup>1</sup>, Youwang Hu<sup>1,2\*</sup>, Ji-an Duan<sup>1</sup>*

1 State Key Laboratory of High Performance and Complex Manufacturing, College of Mechanical and Electrical Engineering, Central South University, Changsha, Hunan 410083, China

2 Science and Technology on Reliability Physics and Application Technology of Electronic Component Laboratory, Guangzhou 510610, China

\*Corresponding author: [huyw@csu.edu.cn](mailto:huyw@csu.edu.cn)

(Including Videos S1~S3 and Figures S1-S7 in the Supporting Information)

### Supporting Videos:

**Video S1.** Curvilinear motion of the droplet.

**Video S2.** Manipulation of multiple droplets by triple rotating CSTFs.

**Video S3.** Microreaction orderly triggered by the CSTF.

## Supporting Figures

**Figure S1** demonstrates the droplet manipulation platform. The laser routes were designed by computer aided design. All droplets were actuated by rapid and selective laser irradiation on lubricant-infused surface. A CMOS was placed on the side view to capture the droplet motion in  $x$  direction. Another CCD was placed on the top view to capture the droplet motion in  $y$  direction. Thermal imager was placed on the top of the surface to capture the temperature field.

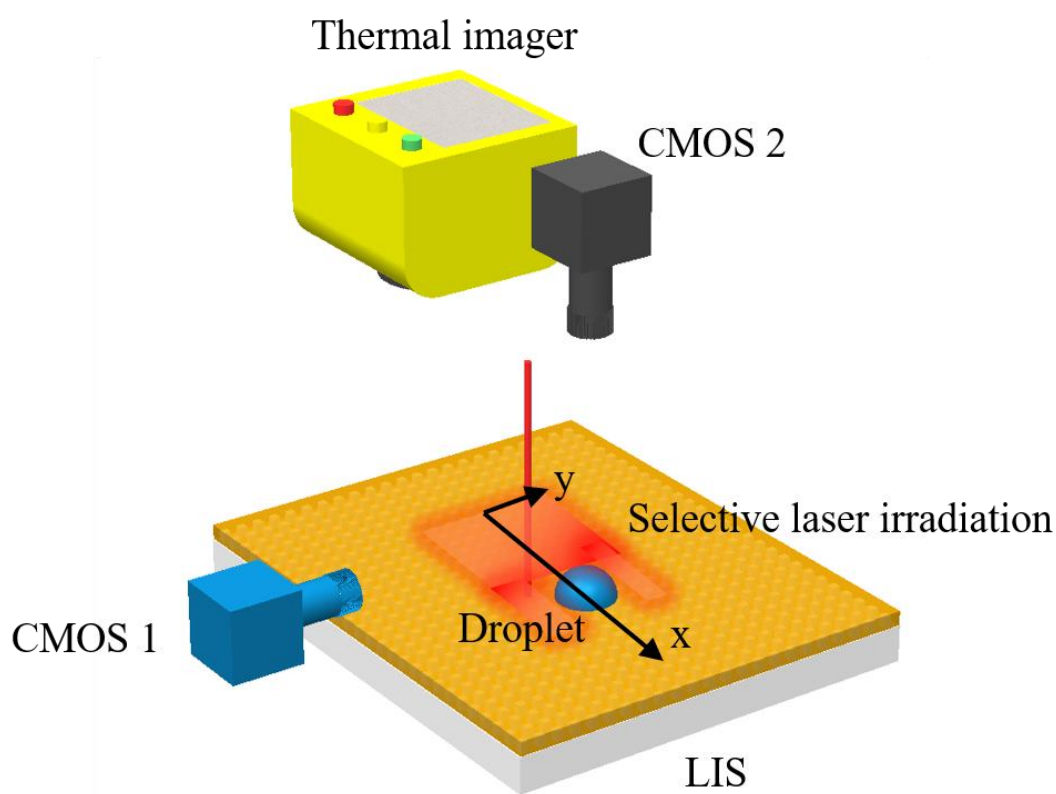


**Figure S1.** Droplet manipulation platform.

**Figure S2** demonstrates the droplet motion actuated by direct laser irradiation control method and selective laser irradiation. As shown in **Figure S2(a)**, the circular laser spot caused the deviation of the droplet from the designed route. Meanwhile, the rapid and selective laser irradiation induced C-shape temperature field, which actuated

the off-track droplet to the designed route, as shown in **Figure S2(b)**.

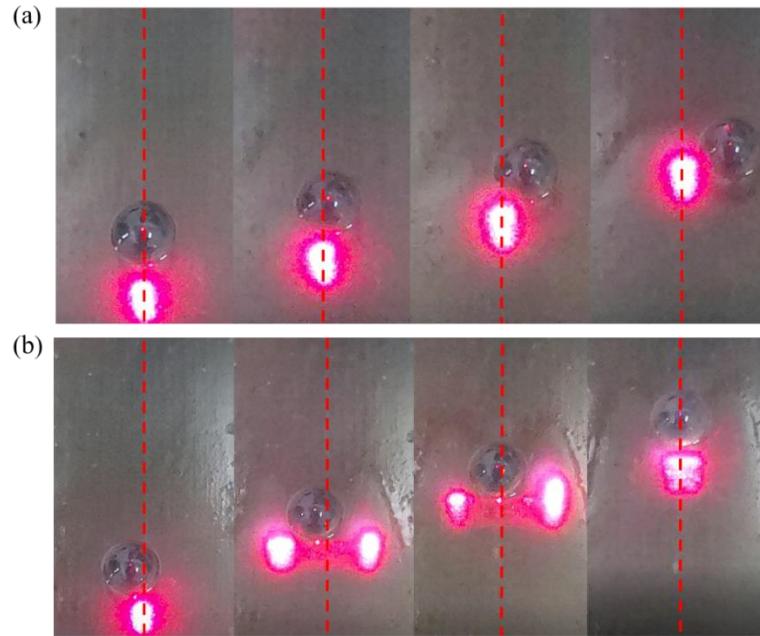


**Figure S2.** Droplet manipulation with different methods. (a) Droplet motion actuated by direct laser irradiation. (b) Droplet motion actuated by rapid and selective laser irradiation.

**Figure S3(a1, b1, c1)** demonstrates the droplet temperature in  $x$  direction with  $u = 0.79, 0.97, 1.22\text{mm/s}$ . The temperature increased gradually until the temperature balance time  $t_T$ .  $t_T$  was estimated as 6.85, 6.78 and 7.18s respectively for different driving velocities. **Figure S3(a2, b2, c2)** displays the droplet temperature in  $y$  direction. The droplet temperature was slightly changed due to the deviation of the droplet. Finally, the droplet temperature in  $y$  direction was balance when the droplet moved unidirectionally.

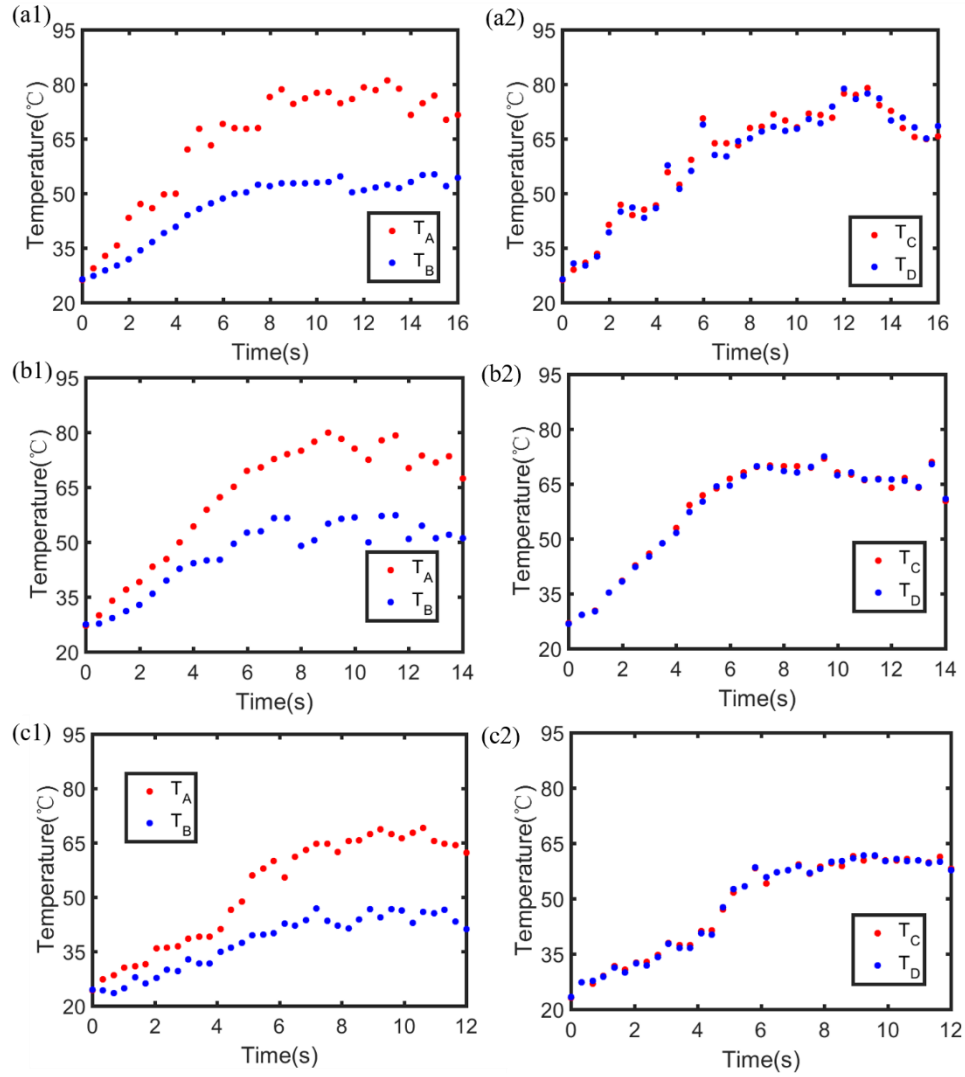


**Figure S3.** Droplet temperature at different points with  $u = 0.79, 0.97, 1.22$  mm/s. (a1-c1) Droplet temperature at A and B point with  $u = 0.79, 0.97, 1.22$  mm/s. (a2-c2) Droplet temperature at C and D point with  $u = 0.79, 0.97, 1.22$  mm/s.

Corresponding to **Figure 3(c, d)** and **Figure S3**,  $\Delta T_s$  during balance time with difference driving velocity were calculated.  $\Delta T_{x,s} = 18.52, 22.14, 19.34, 21.46$  °C corresponding to  $u = 0.61, 0.79, 0.97, 1.22$  mm/s. In addition, it was noting that  $\Delta T_{y,s} = 0.1, -1.13, -0.41, -0.14$  °C. It indicated that  $F_M$  was a constant with different  $u$  after the transition time  $t_T$ .

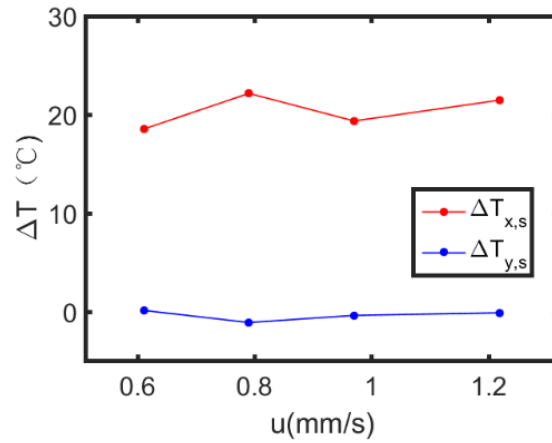


**Figure S4.** Steady temperature difference with different driving velocities.

**Figure S5** demonstrates the relationship between driving velocity  $u$  and steady velocity  $v_s$  of 10  $\mu\text{L}$  droplet.

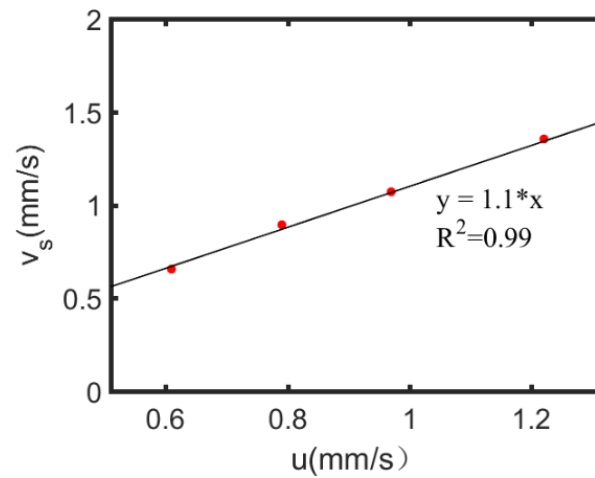


**Figure S5.** Relationship between driving velocity  $u$  and steady velocity  $v_s$ .

**Figure S6** demonstrates the repeatability of the droplet motion. A 10  $\mu\text{L}$  water droplet was driven in 6 cycles with  $u = 0.97$  mm/s. **Figure S6(a)** demonstrates the driving laser position based on the equation (6). The laser scanned for 1.72 s at the original position. Subsequently, it moved uniformly with  $u = 0.97$  mm/s. The designed

distance  $L = 12$  mm. While the CSTF position  $x_c$  reached 12 mm, the CSTF turned back and actuated the droplet reversely. It was noting that the droplet contact diameter  $d$  should be considered for the reverse driving position. Therefore, the maximum position of the CSTF was  $L + d = 15.1$  mm.

Correspondingly, the droplet position was under control. As shown in **Figure S6 (b)**, the droplet was accelerated gradually until the transition time  $t_T$ . Subsequently, the droplet moved uniformly before the CSTF moved reversely. Similarly, the droplet was actuated reversely by the driving laser to the original position. The displacement error is  $\pm 0.80$  mm during the whole process. Herein, the droplet position showed good repeatability.

**Figure S6(c)** exhibits the average velocity of positive and reverse direction of each cycle. The average velocity  $v_{avg} = 0.91 \pm 0.09$  mm/s, while the reverse average velocity =  $-0.92 \pm 0.07$  mm/s. For each cycle, the fluctuation of  $v_{avg}$  could be ignored. Moreover, it was noting that the positive and negative average velocity were equal in absolute value, which meant the droplet average velocity was also repeatable for 6 cycles.

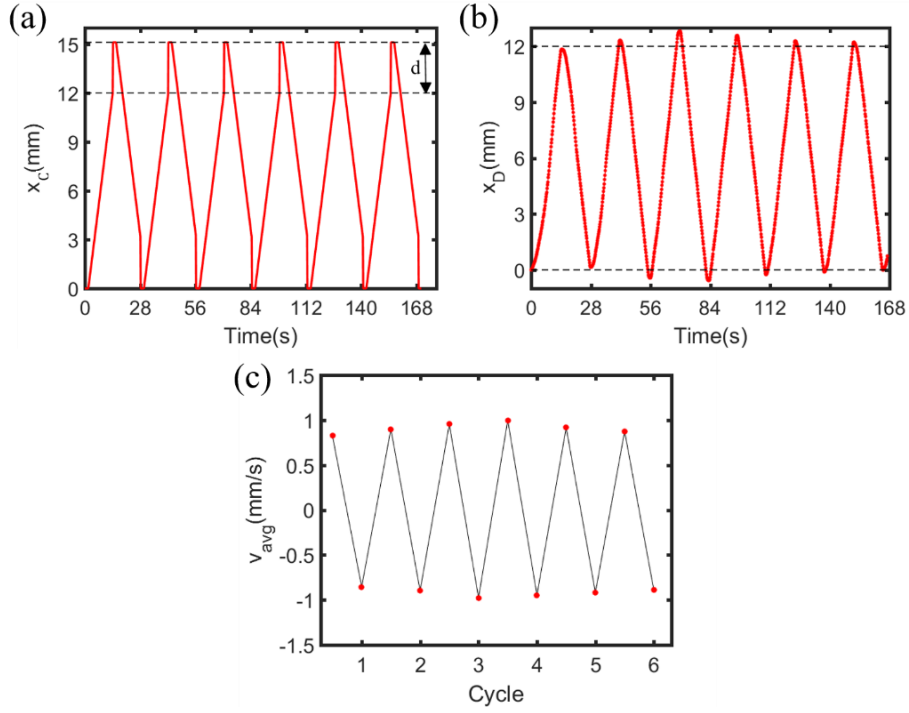


**Figure S6.** Repeatability of droplet motion. (a) Position of the CSTF for 6 cycles with driving velocity  $u=0.97\text{mm/s}$ . (b) Corresponding droplet motion for 6 cycles. (c) Droplet average velocity for 6 cycles.

The thermal effect will lead to the water evaporation. Here, the evaporation rate(ER) can be estimated by:  $ER \approx 1 - \left(\frac{d_1}{d_0}\right)^2 \frac{h_1}{h_0}$ . For instance, **Figure S7(a)** and **(b)** demonstrate the droplet motion at the original position and the terminal position respectively.  $L$  was the designed distance about 12 mm. The droplet size was captured from the pictures. The driving velocity  $u = 0.61 \text{ mm/s}$ ,  $d_0 = 3.15 \text{ mm}$ ,  $d_1 = 3.17 \text{ mm}$ ,  $h_0 = 1.94 \text{ mm}$ ,  $h_1 = 1.74 \text{ mm}$ , then  $ER \approx 0.09$ .

In addition, ER was estimated for different driving velocities. As shown in **Figure S7(c)**, with the increasing of the driving velocity from 0.61 to 1.22 mm/s, ER = 0.09, 0.07, 0.05 and 0.03 respectively. There are two explanations for such phenomenon. On

one hand, the evaporation time reduced with the increasing of driving velocity. On the other hand, the larger driving velocity  $u$  reduced the heat density on the LIS. As a result, the evaporation rate of the droplet can be ignored in a short time if the driving velocity is not less than 0.97 mm/s ( $ER \leq 0.05$ ).

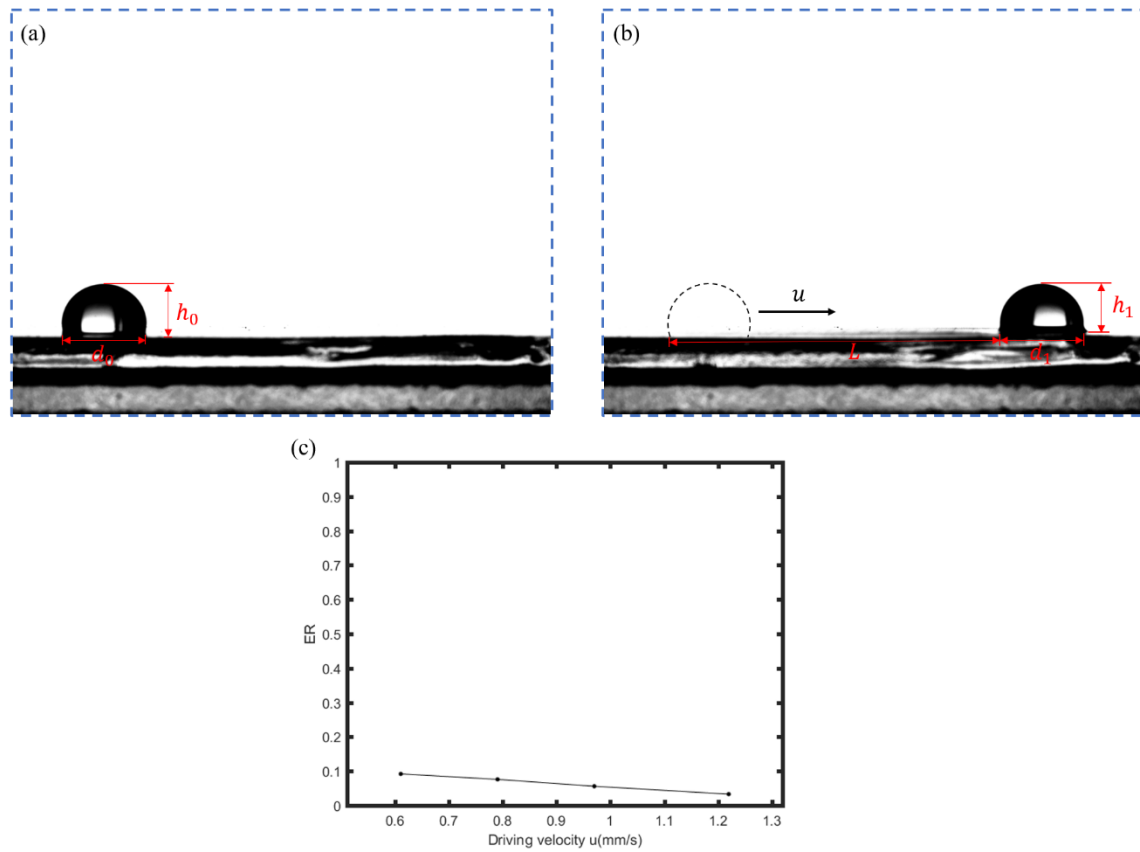


**Figure S7.** Estimation of evaporation of the droplet. (a) Droplet at the original position. (b) Droplet at the terminal position. (c) Evaporation rate (ER) of droplet with different driving velocities.